Turbulent heat transfer to power-law fluids in helical passages

B. K. Rao
College of Engineering, Idaho State University, Pocatello, ID, USA

The fully developed turbulent Fanning friction factors and Nusselt numbers for purely viscous power-law non-Newtonian fluids in helical coils were measured experimentally. The flow passage is about 600 hydraulic diameters long. The test section wall was heated by passing direct electric current through it, yielding constant peripheral wall temperature and constant heat flux per unit length along the flow direction.

For turbulent power-law fluid flows through helical coils, over the range of the coil-to-tube diameter ratio from 10 to 26, the generalized Reynolds number (Re*) from 25,000 to 50,000, the Prandtl number from 6 to 14, and the power-law exponent (n) from 0.78 to 1, improved correlations for friction factor-prediction and a new correlation for Nusselt number are proposed. Other than space saving, helical coils do not offer any advantages over a straight tube for heat-exchanger applications involving turbulent flow of Newtonian or power-law non-Newtonian fluids.

Keywords: power-law fluids; helical coils; heat transfer; friction factor

1. Introduction

Helical coils are extensively used in chemical reactors, food processing industries, and medical equipment such as kidney dialysis machines. The fluids transported in such applications are often non-Newtonian. The published information pertinent to the non-Newtonian flows through helical coils is very limited.

Non-Newtonian fluids can be broadly classified into purely viscous power-law fluids (inelastic) and visco-elastic fluids. The governing equations for hydrodynamics and heat transfer of non-Newtonian fluids may be found in Bird et al. (1960) and Skelland (1967).

For simple viscometric flow of a power-law fluid, the shear stress (τ) and shear rate ($\dot{\gamma}$) are related as given below:

$$\tau = K\dot{\gamma}^n = \eta\dot{\gamma} \tag{1}$$

where η is the apparent viscosity. (The rheological constants n and K may be obtained by using Equations 15 and 16 below.) Kozicki et al. (1966) introduced a universal Reynolds number, Re*, such that the laminar friction factor for isothermal flow of non-Newtonian fluids in ducts of arbitrary cross section is given by 16/Re*, where

$$\mathrm{Re}^* = \rho v^{2-n} D_h^n / \{K[(a + bn)/n]^n 8^{n-1}\} \tag{2}$$

The parameters a and b are functions only of the geometry of the flow cross section (Kozicki et al. 1966). The constants a and b for a circular geometry are 1/4 and 3/4, respectively. For Newtonian fluids ($n = 1$, and $\eta = \mu$) flowing through straight pipes, Re* reduces to the well-known Reynolds number, Re ($=\rho v d/\mu$), where μ is the dynamic viscosity and d is the internal diameter of the straight pipe.

Laminar friction factor and heat transfer of power-law fluid flows through straight pipes of circular cross section are not significantly different from those of Newtonian flows. However, turbulent flows (in straight tubes) of power-law fluids are associated with a higher Nusselt number and a lower friction factor compared with those of a Newtonian solvent at any fixed Re*.

Turbulent friction factors for power-law fluid flows in straight channels are well predicted by Dodge–Metzner's equation (Friend and Metzner 1958):

$$f^{-1/2} = 4n^{-3/4} \log_{10}[\mathrm{Re}^* f^{1-n/2}] - 0.4n^{-1.2} \tag{3}$$

which reduces, in the limit as n tends to unity, to the well-known Karman–Nikuradse equation for the Newtonian turbulent fully developed friction factor in smooth straight channels. The turbulent friction factor of power-law fluids depends on Re*, n, and the pH value of the fluid (Cho and Hartnett 1982). As the polymer concentration in a Newtonian solvent is increased, the solution (power-law fluid) viscosity (hence, the Prandtl number) increases and the n value monotonically decreases. The turbulent pressure drop for power-law fluid flow in a straight pipe is greater than that for a Newtonian solvent when compared at any fixed mass flow rate. However, at any given Re*, the turbulent friction factor for power-law fluid flow in a straight pipe decreases from that of the Newtonian solvent as n decreases (Cho and Hartnett 1982; Friend and Metzner 1958; Hartnett and Rao 1987; Hartnett et al. 1986; Metzner 1965).

Shah and Johnson (1981) reviewed the available predictions for fully developed turbulent Nusselt number for Newtonian flows in straight circular and noncircular channels. One of the most commonly used prediction for turbulent Newtonian fully developed Nusselt number is Petukhov's:

$$\mathrm{Nu} = (\tfrac{1}{2} f\ \mathrm{Re}\ \mathrm{Pr})/[1.07 + 12.7(f/2)^{1/2}(\mathrm{Pr}^{2/3} - 1)] \tag{4}$$

in the range $0.5 < \mathrm{Pr} < 200$, and $10^4 < \mathrm{Re} < 5 \times 10^6$.

It is also experimentally verified that the turbulent fully developed Nusselt number for power-law fluids in straight channels increases with decreasing n value at any fixed Re*. The turbulent Nusselt number for power-law fluid flows through straight channels may be estimated using some of the

Address reprint requests to Professor Rao at the College of Engineering, Idaho State University, Pocatello, ID 83209, USA.

Received 1 February 1993; accepted 12 July 1993

available established predictions (for H1 thermal boundary condition):

Friend and Metzner (1958):

$$\mathrm{Nu} = (\tfrac{1}{2} f\ \mathrm{Re}_a\ \mathrm{Pr}_a)/[1.2 + 11.8(f/2)^{1/2}(\mathrm{Pr}_a - 1)\mathrm{Pr}_a^{1/3}] \quad (5)$$

$$\mathrm{Pr}_a\ \mathrm{Re}_a^2\ f > 10^5$$

Yoo and Hartnett (1974):

$$\mathrm{Nu} = 0.0152(\mathrm{Re}_a)^{0.845}(\mathrm{Pr}_a)^{1/3} \quad (6)$$

$$0.2 < n < 0.9, \quad 3{,}000 < \mathrm{Re}_a < 90{,}000$$

Hartnett and Rao (1987):

$$\mathrm{Nu} = (0.0081 + 0.0149n)(\mathrm{Re}_a)^{0.8}(\mathrm{Pr}_a)^{0.4} \quad (7)$$

Pr_a and Re_a are the Prandtl number and Reynolds number based on apparent viscosity, η. Both Equations 5 and 6 were proposed for heat transfer to power-law fluids in circular pipes. Equation 5 yields predictions within ± 25 percent of the available data. Equation 6 is simpler but does not agree with the well-established Dittus–Boelter equation or with the Petukhov equation for the Newtonian case. Equation 7 predicts the available data for circular and rectangular geometries with an accuracy of ± 20 percent. In the limit, as n approaches unity, Equation 7 reduces to the well-known Dittus–Boelter equation for turbulent Newtonian Nusselt number.

Turning next to helical flow passages, some experimental studies (Sreenivasan and Strykowski 1983) indicate that when a Newtonian fluid flowing through a straight tube under turbulent conditions is passed through a helical coil, partial relaminarization occurs; the extent to which the relaminarization takes place depends on the range of the Reynolds number. It is well known that Newtonian flows exhibit increased heat transfer and pressure drop in helical coils (due to induced secondary flows) compared with those in straight pipes at any fixed flow rate. Numerous studies were reported on the Newtonian friction factor and heat transfer in curved pipes for laminar flow, while relatively fewer papers (e.g., Ito 1959; Schmidt 1967; Srinivasan et al. 1970) have dealt with turbulent flow of Newtonian fluids in coils. Some of the available correlations for turbulent Newtonian friction factor in helical coils are as follows:

Ito (1959):

$$f(D/d_i)^{1/2} = 0.00725 + 0.076[\mathrm{Re}\,(d_i/D)^2]^{-1/4} \quad (8)$$

for $0.034 < \mathrm{Re}\,(d_i/D)^2 < 300$

Srinivasan et al. (1970):

$$f(D/d_i)^{1/2} = 0.084[\mathrm{Re}\,(d_i/D)^2]^{-1/5} \quad (9)$$

for $\mathrm{Re}\,(d_i/D)^2 < 700$ and $7 < (D/d_i) < 104$

where d_i and D are the internal diameter of the tube and the mean diameter of the coil, respectively. Equations 8 and 9 agree with each other very well and show good agreement (within ± 10 percent) with experimental data for water (Rogers and Mayhew 1964) and with numerical predictions by Patankar et al. (1975). Rogers and Mayhew (1964) recommend the following for predicting nonisothermal friction factor in helical coils:

$$f_{\text{nonisothermal}} = f_{\text{isothermal}}\,(\mathrm{Pr}_m/\mathrm{Pr}_w)^{-1/3} \quad (9a)$$

where $f_{\text{isothermal}}$ is calculated using Equation 8.

Schmidt (1967) proposed the following prediction (with the largest applicable range) for the Newtonian turbulent fully developed Nusselt number in helical coils (Nu_c) for H1 thermal boundary condition:

$$(\mathrm{Nu}_c/\mathrm{Nu}_s) = 1 + 3.6[1 - (d_i/D)](d_i/D)^{0.8} \quad (10)$$

for $20{,}000 < \mathrm{Re} < 150{,}000$ and $5 < D/d_i < 84$, where Nu_s refers to the turbulent Nusselt number in straight pipes. It may be concluded that the turbulent hydrodynamic and heat transfer performance of Newtonian fluids in helical coils may be predicted with reasonable accuracy. In contrast, the

Notation

a	Constant (see Equation 2)
b	Constant (see Equation 2)
c_p	Fluid specific heat, J/(kg K)
d	Straight tube internal diameter, m
d_i	Coil tube internal diameter, m
D	Helical coil mean diameter, m
D_h	Test section hydraulic diameter, m
h	Heat transfer coefficient $= \dot{q}''/(T_{wi} - T_b)$, W/(m² °C)
H1	Thermal boundary condition referring to constant axial wall heat flux with constant peripheral temperature
H2	Thermal boundary condition referring to axially and peripherally uniform and constant wall heat flux
I	Direct electric current through the coil, Amp
k_f	Fluid thermal conductivity, W/(m K)
K	Consistency index, kg s^{n-2}/m
L	Distance between adjacent pressure taps, m
L'	Test section length, m
n	Power-law exponent
$\dot{q}''$	Heat flux at the inner wall $= VI/(\pi d_i L')$, W/m²
T_b	Fluid bulk temperature, °C
T_{wi}	Inner wall temperature, °C
T_{wo}	Outer wall temperature, °C
v	Fluid mean axial velocity, m
V	Voltage drop across coil, Volt

Dimensionless quantities

De	Dean number $= \mathrm{Re}^*\,(d_i/D)^{1/2}$
f	Fanning friction factor $= \tau_w/(1/2\rho v^2)$
Nu	Nusselt number $= hd_i/k_f$
Pr	Prandtl number $= \mu c_p/k_f$ (for Newtonian fluids)
Pr*	Generalized Prandtl number $= \rho v d c_p/(k_f \mathrm{Re}^*)$
Pr_a	Generalized Prandtl number $= \eta c_p/k_f$
Re	Reynolds number $= \rho v d/\mu$ (for Newtonian fluids)
Re*	Generalized Reynolds number (see Equation 2)
Re_a	Reynolds number based on apparent viscosity $= \rho v d/\eta$

Greek symbols

$\dot{\gamma}$	Shear rate for viscometric flow, s^{-1}
η	Apparent viscosity of power-law fluid, kg/(m s)
μ	Dynamic viscosity of Newtonian fluid, kg/(m s)
ρ	Density of test fluid, kg/m³
τ	Shear stress, Pa

Suffixes

a	Based on apparent viscosity
c	Refers to helical coil
m	At mean bulk value; measured quantity
p	Predicted
s	Refers to straight tube
w	At the test section wall

information on turbulent behavior of power-law non-Newtonian fluids in helical coils is extremely limited.

A few results are available for turbulent friction factor of power-law fluid flows through helical coils:

Mishra and Gupta (1979):

$$f = 0.079(\mathrm{Re}_a)^{-1/4} + 0.0075\,(d_i/D)^{1/2} \qquad (11)$$

for $0.02 < [0.079(\mathrm{Re}_a)^{-1/4}](D/d_i)^{1/2} < 0.04$ and $9 < D/d_i < 25$

Rajasekharan et al. (1970):

$$f = 0.079n^{-5}(\mathrm{Re}_a)^{\alpha} + 0.012(d_i/D)^{1/2} \qquad (12)$$

for $6{,}000 < \mathrm{Re}_a < 30{,}000$ and $10 \le (D/d_i) < 27$

where $\alpha = 2.63/(10.5)^n$

Both Equations 11 and 12 have about the same level of accuracy and agree with the well-known Blasius equation, in the limit, when $n = 1$ and D tends to ∞.

For the optimal design of a compact heat exchanger (which usually employs helical coils), it is very important (at least in ground applications) to consider the quantity "heat transfer per unit pumping power." No information is available on turbulent heat transfer behavior of power-law non-Newtonian fluids in helical coils. This experimental study was undertaken to assess the relative performance of a helical coil to that of a straight tube for heat-exchanger applications involving power-law fluids.

2. Experimental setup and procedure

The three stainless steel helical coils used in this study were custom manufactured by a local company. These coils were made by carefully bending straight tubes that were filled with fine sand (to minimize the wall-thinning). The variation in the measured wall thickness of the coils is within 1 percent of the nominal thickness of the tube. The parameters of the helical coils studied are given in Table 1. The schematic of flow loop is shown in Figure 1. The flow loop consists of a 55-gallon plastic reservoir, a positive displacement pump (to minimize mechanical degradation of the polymer chains), helical coils, and a heat exchanger. A sharp entrance is provided at the beginning of the test section such that the flow develops from the entrance. Plumbing connections were made in such a way that the test fluid could be pumped through one coil at a time. Only PVC piping and valves were used in the entire flow loop to minimize any possible chemical reaction between the test fluid and various components of the flow loop. All three coils were mounted parallel to one another on a console in such a manner that all the instrumentation for pressure drop and

Table 1 Parameters of the helical coils

Parameter	Range
Coil	
Mean diameter	98 to 247 mm
Number of turns	8 to 20
Pitch	19.50 mm
Tube	
Inside diameter	9.35 mm
Outside diameter	12.70 mm
Length	6.70 m

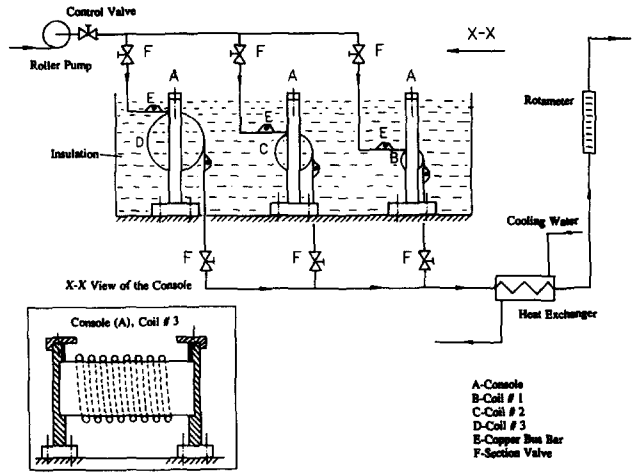

Figure 1 Schematic of flow loop

temperature could be installed near the coils. Each coil was instrumented with some 23 thermocouples (copper constantan, AWG 30) and seven pressure taps (at a distance of $D/2$ from the axis of the coil) at different axial positions. The thermocouple junctions were held to the outer wall by insulating cement (copper oxide), and the insulated thermocouple wire was laid out along the isotherms for a length of at least 30 wire diameters to eliminate heat-conduction error. The test-section outer wall was insulated with fiberglass wool, and the coil was enclosed in a wooden box.

Distilled water was used as a Newtonian fluid. The test fluid was prepared in the plastic reservoir by dissolving polymer powder (of known weight) in distilled water at room temperature, employing only hand stirring (to minimize mechanical degradation). The polymer used to prepare power-law fluids in this study was Carbopol 934 (produced by B.F. Goodrich Chemicals Inc). The polymer used came from a single batch. All three coils were connected, using individual on–off switches and copper bus bars (6.25 mm thick and 10 cm wide), in parallel to a DC power supply. A precision shunt resistance was connected in series with the power supply. Heating of the test section starts from the entrance.

After turning on the flow through the test section, all the air bubbles were vented before turning on the power supply for heating the helical coil wall. The heat input was gradually increased until the temperature of the heated inner wall was about 3°C above the test-fluid bulk temperature (at about 100 hydraulic diameters from the entrance of the coil). All the thermocouple readings (outer wall temperature distribution, and fluid bulk temperatures at inlet and outlet), pressure drop in the fully developed region, voltage drop across the coil (V), and mass flow rate were taken for each run after thermal equilibrium was reached.

The inner wall temperature was calculated using the one-dimensional (1-D) heat-conduction approach. The fluid bulk temperature at any axial position was obtained by linearly interpolating between the fluid bulk temperatures at the entrance and the exit. For the aqueous polymer solutions studied here, all the physical properties (except viscosity) were taken to be the same as for water (Lee et al. 1981).

A calibrated rotameter was used to monitor the flow rate. Actual flow rates were measured using a stop watch and weighing the exiting test fluid collected in a measuring tank. The direct electric current (I) through the coil was calculated using the measured voltage drop across the shunt resistance.

Measurement of the fluid bulk temperatures combined with the measured mass flow rate provided an independent check on the heat input rate (*VI*), and the deviation of the rate of electrical energy input from the rate of enthalpy gained by the test fluid was found to be within ± 2 percent.

The pressure drop (Δp) was measured using a calibrated differential pressure transducer (DP cell). The electrical output (mV) of the transducer used varies linearly (throughout its full range from 0 to 1270 mm water column) with the input Δp. Plumbing connections were made in such a manner that one DP cell is adequate to measure Δp between all pairs of adjacent pressure taps. The flow boundaries were assumed to be smooth. The peripherally and axially averaged wall shear stress, τ_w (at midpoints between adjacent pressure taps), was then calculated as shown below:

$$\tau_w = d_i \Delta p/(4L) \tag{13}$$

where L is the distance between adjacent pressure taps.

The test-fluid steady shear viscosity was measured at room temperature using a capillary viscometer, a Brookfield viscometer, and a Bohlin rheogoniometer. The shear stress (τ) was measured as a function of shear rate ($\dot{\gamma}$), and a parabolic equation was fitted in the range of τ_w measured (between the pressure taps) in the test section as given below:

$$\ln \tau = a_0 + a_1[\ln \dot{\gamma}] + a_2[\ln \dot{\gamma}]^2 \tag{14}$$

The power-law exponent, consistency index, and apparent viscosity were calculated as follows:

$$n = d[\ln \tau]/d[\ln \dot{\gamma}] = a_1 + 2a_2[\ln \dot{\gamma}] \tag{15}$$

$$K = \exp [a_0 - a_2(\ln \dot{\gamma})^2] \tag{16}$$

$$\eta = \tau/\dot{\gamma} \tag{17}$$

The characteristic curves (η as a function of $\dot{\gamma}$) are shown in Figure 2. The test fluid concentrations were 250, 500, and 1000 wppm (parts per million by weight), for which the average values of n are 0.978, 0.804, and 0.758, and the average values of K (at $\dot{\gamma} = 10^4$/s) are 1.1×10^{-3}, 7.7×10^{-3}, and 1.3×10^{-2}, respectively. The aqueous polymer solutions were neutralized, in order to obtain lower values of n (power-law index), by adding sodium hydroxide solution (10 percent strength) until the pH value reached about 7.2. The test fluid rheology was measured before and after each test run to monitor the polymer degradation, and the variation was less than ± 2 percent. No temperature correction was applied for viscosity, since the wall-to-fluid-bulk temperature difference is small.

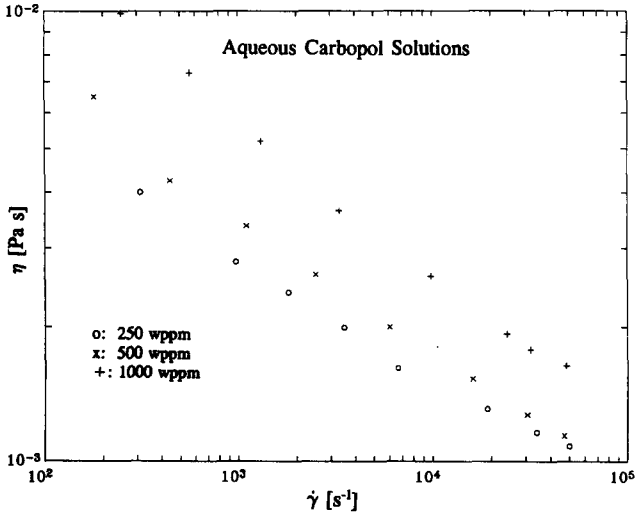

Figure 2 Characteristic curves for aqueous polymer solutions

For each experimental run, a fresh batch of solution was prepared. After completing a set of runs with the same concentration of the polymer, and before starting another set of runs (with a different concentration), the test section was flushed with tap water and then with distilled water for several minutes. The cleanliness of the flow passage was monitored by checking the pressure drop and heat transfer data for distilled water flow.

3. Results and discussion

The pressure drop and heat transfer measurements were carried out simultaneously. All of the present experimental friction factors and Nusselt numbers were obtained in hydrodynamically and thermally fully developed regions. For calibration of the system, turbulent pressure drop and heat transfer were measured for distilled water flow through the coils. The present friction factor data (for $18{,}000 < \mathrm{Re} < 62{,}000$, and $\mathrm{Pr} \sim 5.5$) for water were found to be within ± 10 percent of the values predicted using Equations 8 and 9.

The critical Reynolds number, Re_c, for the helical coils varied from 7,000 to 10,000 for water ($n = 1$) and from 4,000 to 7,400 for the power-law fluids ($0.78 \leq n < 1$). This observation is in agreement with some of the available results (Rajasekharan et al. 1970). Not much is known about the relaminarization of non-Newtonian flows in helical coils. Based on the measured pressure drop and heat transfer in the coils, it is believed that the present results are obtained in the turbulent flow regime. In this experimental investigation, the hydrodynamic entrance length in helical coils for turbulent power-law fluid flow was found to be about the same as that for Newtonian fluids. With relatively higher concentrations of the polymer, even lower values of the power-law exponent, n, can be obtained. However, in such cases the positive displacement pump was only capable of achieving maximum flow rates such that the corresponding Reynolds numbers were not considerably greater than the critical Reynolds number. As a result, the study of turbulent flow of these fluids was limited to the range $0.76 \leq n < 1$.

The appropriate dimensionless number for characterizing the helical flows is the Dean number, De. The definition of the Dean number is the same for Newtonian as well as non-Newtonian fluids except that in the case of non-Newtonian fluids, Re* replaces Re. The measured fully developed turbulent friction factors for Carbopol solutions in a typical coil are shown as a function of De in Figure 3. It can be seen from

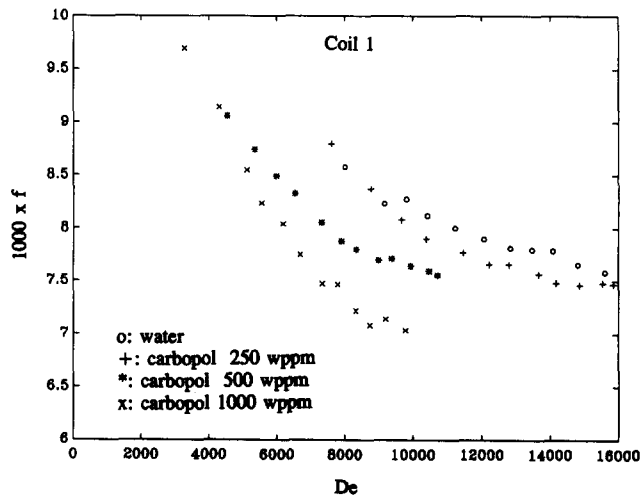

Figure 3 Measured fully developed turbulent Fanning friction factors versus Dean number for aqueous polymer solutions

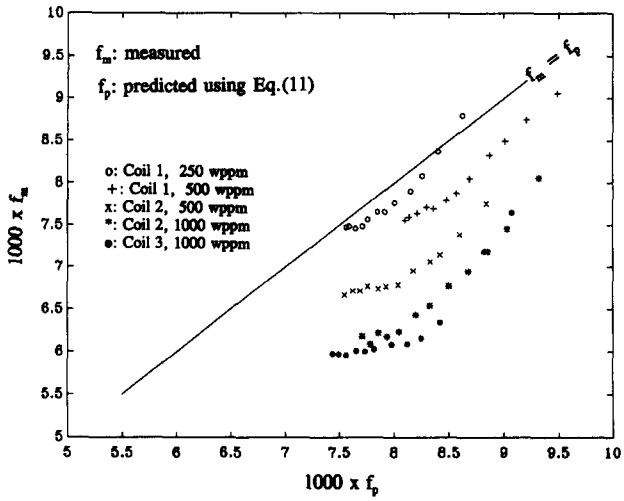

Figure 4 Measured fully developed turbulent friction factors versus predicted friction factors for aqueous polymer solutions

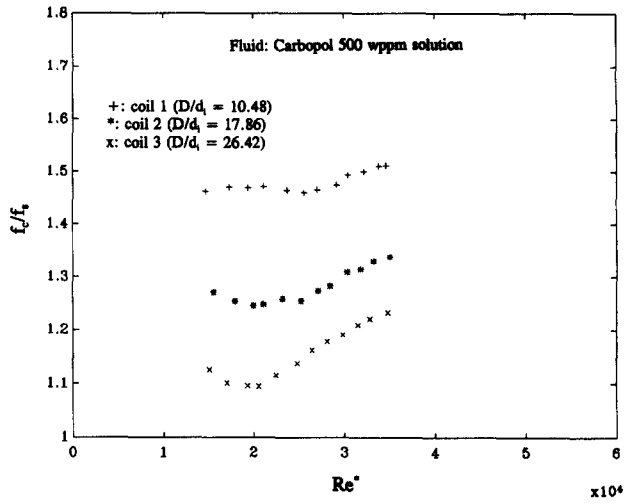

Figure 6 Ratio of measured friction factor in helical coil to that estimated in straight tube as a function of Re*

Figure 3 that the turbulent friction factor of power-law fluids in helical coils increases with decreasing n value, at any fixed De (or Re*). Figure 4 makes a graphical comparison of the present measured friction factors (f_m) with the predicted values (f_p) using Equation 11. From Figure 4 it is apparent that Equation 11 overestimates the present turbulent friction factor in helical coils, and the deviation ($f_p - f_m$) increases with increasing ratio D/d_i and decreasing n value.

The published well-established correlations for the fully developed non-Newtonian turbulent friction factor in helical coils are relatively fewer, and most of them are not expressed in terms of De. In light of this, in this paper, Re* is used to compare the present results with those in the literature and to estimate the relative performance of a coil to a straight tube (for power-law fluids in particular). The following *improved* correlation is proposed to predict the turbulent friction factor for power-law fluids in coils (for $20{,}000 < \mathrm{Re}^* < 50{,}000$, $0.76 \le n \le 1$, $10 \le D/d_i \le 26$):

$$f = n^{0.4}\{0.079(\mathrm{Re}^*)^{-1/4} + [(d_i/D)^{1.5}/14]\} \qquad (18)$$

The measured values of friction factor are plotted against the predicted values using Equation 18 on Figure 5. The bulk of the present experimental friction factor data lie within a region ± 5 percent of the straight line $f_m = f_p$. Equation 18, in the limit as n approaches unity and D tends to ∞, reduces to the well-known Blasius equation (for the Newtonian fully developed turbulent friction factor in smooth straight pipes).

The ratio of the present experimental turbulent friction factors in helical coils to those estimated in straight tubes (f_c/f_s) is plotted as a function of Re* in Figure 6. The f_s values were predicted using Equation 3. From Figure 6 it can be seen that the ratio (f_c/f_s) increases with decreasing value of D/d_i. This observed increase in f_c/f_s is due to the secondary flows induced in coils. Based on the results shown in Figure 6, it appears that the secondary flow effect is weaker at larger values of D/d_i. The variation in the ratio f_c/f_s, at any fixed D/d_i, was found to be no more than ± 5 percent (for $0.76 \le n \le 1$, $10{,}000 \le \mathrm{Re}^* \le 55{,}000$).

No information on thermal entrance lengths for developing turbulent flows of Newtonian or non-Newtonian fluids through helicals is available. The present experimental turbulent heat transfer results were obtained for **H2** thermal boundary condition (see nomenclature). Distributions of the measured outer-wall temperature and the calculated inner-wall temperature are shown for a typical run in Figure 7. The wall temperature distribution suggests that the present turbulent heat transfer data beyond 30 hydraulic diameters are in the

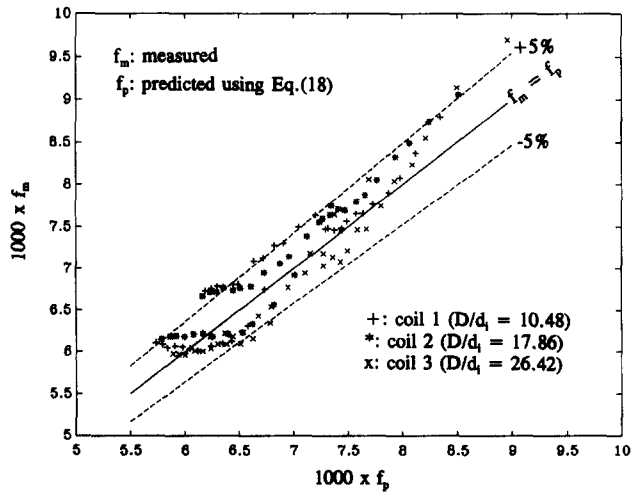

Figure 5 Measured fully developed turbulent friction factors versus predicted friction factors for aqueous polymer solutions

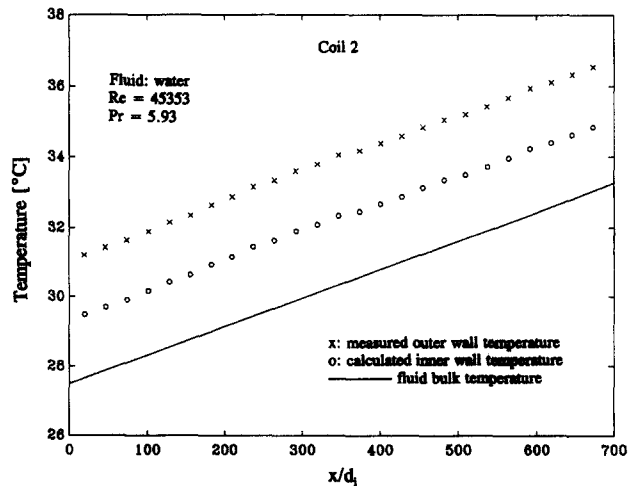

Figure 7 Helical coil wall temperature distribution for a typical run

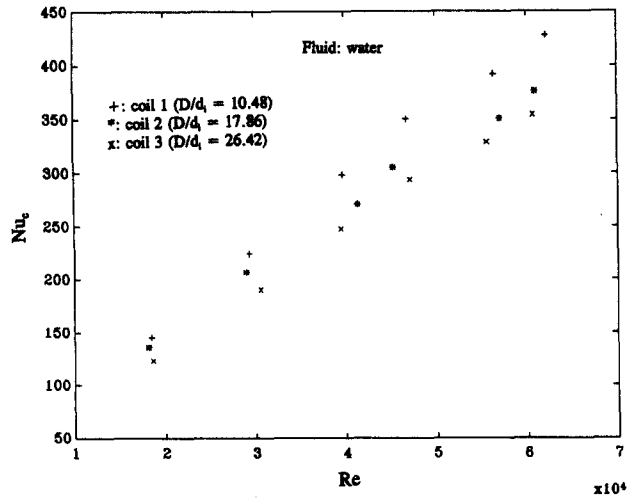

Figure 8 Measured fully developed Nusselt numbers in helical coils as a function of Reynolds number

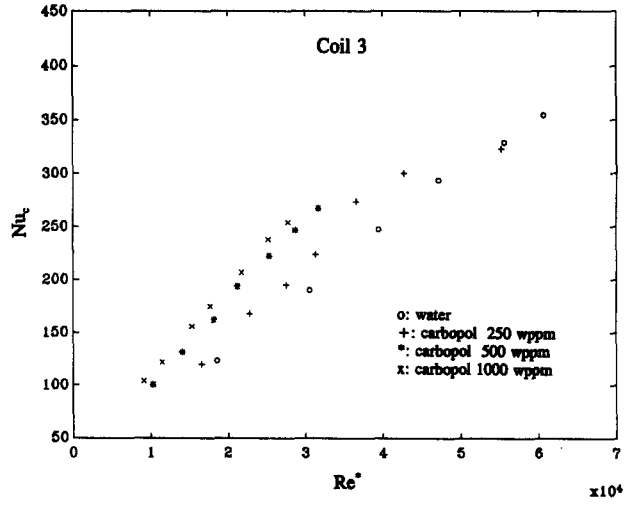

Figure 10 Measured fully developed turbulent Nusselt numbers for aqueous polymer solutions in helical coil as a function of Reynolds number

thermally developed region. In Figure 8, the measured Newtonian turbulent Nusselt numbers in coils (Nu_c) are shown as a function of Re. From Figure 8 it appears that the ratio Nu_c/Nu_s increases with decreasing D/d_i at any fixed Re. The results shown in Figure 8 indicate that the secondary flow effect is weaker at larger values of D/d_i. The measured Nusselt numbers are plotted in Figure 9 against the values predicted using Equation 10. From Figure 9 it can be seen that Equation 10 overpredicts the present Nu_c/Nu_s values. An *improved* correlation is proposed based on the present experimental heat transfer data for water:

$$(Nu_c/Nu_s) = 1 + 1.48(d_i/D)^{1.15} \quad (19)$$

for 15,000 < Re < 63,000 and $10 < d_i/D < 30$. The Nu_s values in Equations 10 and 19 were predicted using Equation 4. The new correlation predicts the present data with an accuracy of ±5.5 percent.

The thermal entrance length for turbulent flow of purely viscous non-Newtonian fluids in a straight circular pipe is about the same as that for Newtonian fluids (Yoo and Hartnett 1974). The wall temperature distribution (not shown here) for turbulent flow of power-law fluids, in the present study, suggests that the thermal entrance length in helical coils is of the same order as that of the Newtonian fluids.

The measured turbulent Nusselt numbers for water and power-law fluids are shown in Figure 10 as a function of Re*. Based on the results shown in Figure 10, the turbulent Nusselt number in coils increases with decreasing n value. This observed heat transfer augmentation is attributed to the induced secondary flows. Figure 11 presents the ratio of the measured turbulent Nusselt numbers in the helical coil (Nu_c) to those estimated in straight pipes (Nu_s, using Equation 7) as a function of Re*. From Figure 11 it can be seen that the ratio Nu_c/Nu_s increases with decreasing n for any fixed D/d_i. This observed increase in heat transfer is attributed to the secondary flows induced in the coil. Some studies (Hsu and Patankar 1982) suggest that decreasing n value dampens secondary flow in helical coils. However, based on the results shown in Figure 11, it appears that the lower the n value, the greater the strength of the secondary flows induced in a helical coil. Present turbulent heat transfer data for power-law fluids suggest that the effect of D/d_i is more pronounced than that of the n value

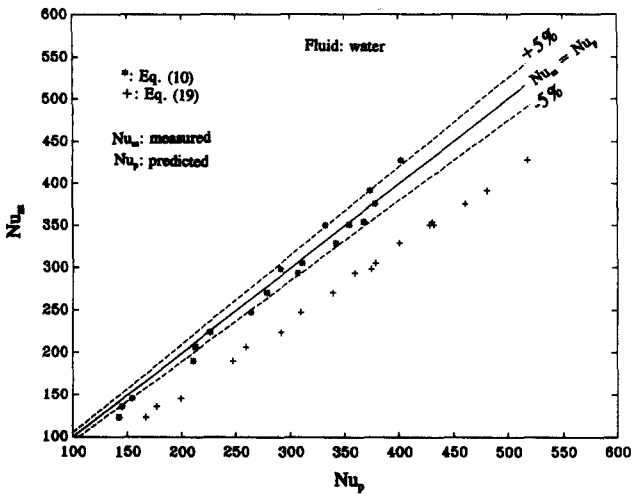

Figure 9 Measured fully developed Nusselt numbers versus predicted Nusselt numbers for turbulent water flow in helical coils

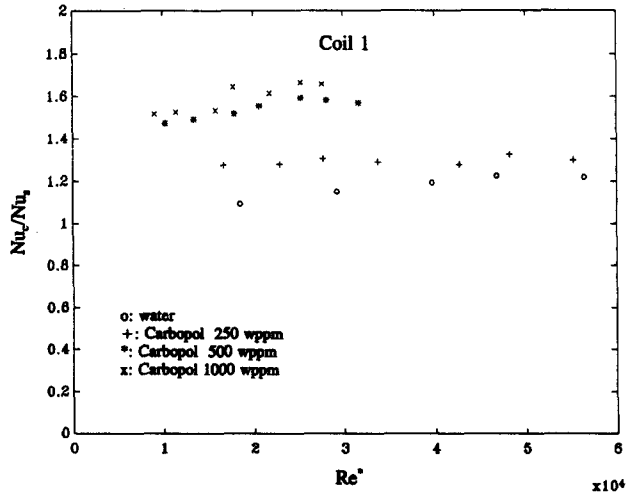

Figure 11 Ratio of measured fully developed turbulent Nusselt number in helical coil to that estimated in straight tube as a function of Reynolds number (for different polymer concentrations)

on the ratio Nu_c/Nu_s. No analytical or experimental results are available with which to compare the present data.

Based on the current results, the following correlation is proposed for predicting turbulent Nusselt number for power-law fluids in helical coils:

$$(Nu_c/Nu_s) = [1 + 2.9(d_i/D)]^{1.15}[0.55 + 0.45\,n]^{-1.25} \quad (20)$$

for $9{,}000 < Re^* < 55{,}000$ and $10 < d_i/D < 30$. Equation 20 fits the present heat transfer results within ± 2 percent. The error analysis (using the root of the sum of the squares method) revealed that the uncertainties in the friction factors and Nusselt numbers in the present study are within ± 6 percent and ± 10 percent, respectively.

The relative performance of a helical coil to a straight tube may be described by the ratio $[(Nu_c/Nu_s)/(f_c/f_s)]$, which is important for the optimal design of a heat exchanger. Present experimental data for water (a Newtonian fluid) and aqueous Carbopol solutions (purely viscous power-law non-Newtonian fluids) have a range for the ratio above from 0.98 to 1.15. These limited experimental data suggest that the ratio above increases slightly with increasing Re^* and with decreasing n, although the effect of these two variables (for $25{,}000 \leq Re^* \leq 50{,}000$ and $0.76 \leq n \leq 1$) is quite small. Within the limits of experimental uncertainties, D/d_i (over the range from 10 to 26) revealed no influence on the ratio $[(Nu_c/Nu_s)/(f_c/f_s)]$. More experimental or analytical results are needed to confirm this observation.

4. Conclusions

(1) The fully developed turbulent friction factors for water in helical coils are in good agreement with the available predictions (Equations 8 and 9);
(2) the measured fully developed turbulent friction factors for power-law fluids in helical coils are overpredicted by Equations 11 and 12;
(3) a new equation is proposed for the turbulent friction factor; it correlates the present experimental data for power-law fluids in coils with an accuracy of ± 5 percent;
(4) the measured fully developed turbulent Nusselt numbers for water are overestimated by Equation 10;
(5) a new correlation is proposed for the turbulent Nusselt number (for **H2** thermal boundary condition) based on the present data for power-law fluids in helical coils; and
(6) the fact that the current ratio $[(Nu_c/Nu_s)/(f_c/f_s)]$ is about unity suggests that, other than space saving, helical coils do not offer any advantages over a straight tube for heat-exchanger applications involving turbulent flow of power-law non-Newtonian fluids.

Acknowledgments

The author acknowledges the financial support from the Office of the Dean, College of Engineering, Idaho State University for carrying out this research.

References

Bird, R. B., Armstrong, R. C., and Hassager, O. 1960. *Dynamics of Polymeric Liquids*, Vol. 1. Wiley, New York

Boyce, B. E., Collier, G. J., and Levy, J. 1969. Hold-up and pressure drop measurements in the two-phase flow of air–water mixtures in helical coils. *Co-current Gas Liquid Flow*. Plenum Press, UK, 203–231

Cho, Y. I. and Hartnett, J. P. 1982. Non-Newtonian fluids in circular pipe flow. *Adv. Heat Transfer*, **15**, 59–141

Friend, W. L. and Metzner, A. B. 1958. Turbulent heat transfer inside tubes and the analogy among heat, mass, and momentum transfer. *AIChEJ*, **4**, 393–402

Hartnett, J. P. and Rao, B. K. 1987. Heat transfer and pressure drop for purely viscous non-Newtonian fluids. *Wärme-und Stoffübertragung*, **21**, 1–7

Hartnett, J. P., Kwack, E. Y., and Rao, B. K. 1986. Hydrodynamic behavior of non-Newtonian fluids in a square duct. *J. Rheol.*, **30**, S45–S59

Hogg, G. W. 1968. The effect of secondary flow on point heat transfer coefficients for turbulent flow inside curved tubes. Ph.D. Thesis, University of Idaho

Hsu, C. F. and Patankar, S. V. 1982. Analysis of laminar non-Newtonian flow and heat transfer in curved tubes. *AIChEJ*, **28**, 610–616

Ito, H. 1959. Friction factors for turbulent flow in curved pipes. *J. Basic Eng.*, **81**, 123–134

Kozicki, W., Chou, C. H., and Tiu, C. 1966. Non-Newtonian flow in ducts of arbitrary cross-sectional shape. *Chem. Eng. Sci.*, **21**, 665–679

Lee, W. Y., Cho, Y. I., and Hartnett, J. P. 1981. Thermal conductivity measurements of non–Newtonian fluids. *Lett. Heat Mass Transfer*, **8**, 255–259

Metzer, A. B. 1965. Heat transfer in non-Newtonian Fluids. *Adv. Heat Transfer*, **2**, 357–397

Mishra, P. and Gupta, S. N. 1979. Momentum transfer in curved pipes, 2, Non–Newtonian fluids. *Ind. Eng. Chem. Proc. Design Dev.*, **18**, 137–142

Mori, Y. and Nakayama, W. 1967. Study on forced convective heat transfer in curved pipes. *Int. J. Heat Mass Transfer*, **10**, 37–59

Mujawar, B. A. and Raja Rao, M. 1978. Flow of non-Newtonian fluids through helical coils. *Ind. Eng. Chem. Proc. Design Dev.*, **17**, 22–27

Patankar, S. V., Pratap, V. S., and Spalding, D. B. 1975. Prediction of turbulent flow in curved pipes. *J. Fluid Mech.*, **67**(3), 583–595

Rajasekharan, S., Kubair, V. G., and Kuloor, N. R. 1970. Flow of non-Newtonian fluids through helical coils. *Indian J. Tech.*, **8**, 391–397

Rogers, G. F. C. and Mayhew, Y. R. 1964. Heat transfer and pressure loss in helically coiled tubes with turbulent flow. *Int. J. Heat Mass Transfer*, **7**, 1207–1216

Schmidt, E. F. 1967. Wärmeübergang und druckverlust in rohrschlangen. *Chem. Eng. Tech.*, **39**, 781–789

Shah, R. K. and Johnson, R. S. 1981. Correlations for fully developed turbulent flow through circular and non-circular channels. *3rd Nat. Heat Transfer Conf.*, HMT-126-81: D-75, India

Skelland, A. H. P. 1967. *Non-Newtonian Flow and Heat Transfer*. Wiley, New York

Sreenivasan, K. R. and Strykowski, P. J. 1983. Stabilization effects in flow through helically coiled pipes. *Exp. Fluids*, **1**, 31–36

Srinivasan, P. S., Nandapurkar, S. S., and Holland, F. A. 1970. Friction factor for coils. *Trans. Inst. Chem. Engrs.*, **48**, T156–T161

Yoo, S. S. and Hartnett, J. P. 1974. Heat transfer and friction factors for purely viscous non-Newtonian fluids in turbulent pipe flow. *5th Int. Heat Transfer Conf.*, **FC5.8**, 218–222